



# Comparison of the Thermal Transitions of Spray-Dried and Freeze-Dried Egg Whites by Differential Scanning Calorimetry

Jin-Hong Zhao<sup>1</sup> · Li-Sha Liu<sup>1</sup> · Shyam S. Sablani<sup>2</sup> · Yi-Jiao Peng<sup>1</sup> · Hong-Wei Xiao<sup>3</sup> · Jie Bai<sup>1</sup> · Hong Guo<sup>1</sup>

Received: 20 October 2019 / Accepted: 10 June 2020 / Published online: 20 June 2020  
© Springer Science+Business Media, LLC, part of Springer Nature 2020

## Abstract

The thermal transitions of spray-dried (SD) and freeze-dried (FD) egg whites containing unfreezable water (i.e., lower water contents) and freezable water (i.e., higher water contents) were measured by differential scanning calorimetry (DSC). For the SD and FD samples containing unfreezable water (0.039–0.282 and 0.043–0.206 g water/g sample (w.b.) in SD and FD samples), the denaturation temperatures ( $T_d$ ) of ovotransferrin and ovalbumin were observed in both the SD and FD samples. However, it was difficult to identify the glass transition temperature ( $T_g$ ) of the egg whites. The  $T_g$  was only detected in SD egg whites with low water contents (0.039–0.093 g water/g sample (w.b.)). For the SD and FD samples containing freezable water (0.32–0.72 and 0.31–0.73 g water/g sample (w.b.) in SD and FD samples), the glass transitions were not detected, and only the freezing points ( $T_F$ ) and the end point of freezing ( $T_m'$ ) were observed. The unfreezable water content and the corresponding characteristic end point of freezing ( $T_m'$ )<sub>u</sub> of the SD samples were both greater than those of the FD samples. The heat denaturation of egg white proteins and different protein solubility (water-binding capacity) may cause the different thermal transitions between SD and FD egg whites. But the Guggenheim-Anderson-de Boer (GAB) monolayer water contents of the SD and FD egg white powders were similar. The results are useful for selecting the optimal process and storage conditions for dried and frozen egg whites.

**Keywords** Glass transition temperature · Water activity · Spray-drying · Freeze-drying · Egg white · Differential scanning calorimetry (DSC)

## Introduction

The hen egg is a rich source of high-quality proteins, lipids, minerals, carbohydrates, and vitamins. Egg white is well known for its functionalities, such as foaming, emulsifying, and gelling. Therefore, egg white is utilized in bakery foods, salad dressing, confectionery products, and many convenience foods (Ayadi et al. 2008). Recently, instead of using shell eggs as an ingredient, powdered, pasteurized liquid, or frozen eggs are being used extensively in the food industry.

Dried egg powders not only have functional properties, but also some advantages, including with respect to transportation, storage, handling, and microbiological safety (Koç et al. 2012).

Spray- and freeze-drying are conventional methods used in the food industry for concentrating liquids or for converting them into powder or flour. Spray-drying is the most popular drying technology used to prepare protein powder. The liquid feed is converted to a powder by an atomizer of the spray dryer and placed in contact with hot air, which may change the conformation of the materials during the spray-drying process (Chen et al. 2012). Freeze-drying utilizes the mechanism of ice sublimation under lower pressure and can maintain good food quality. Additional advantages of freeze-drying include suitability in drying heat-sensitive materials and good rehydration capacity of dried foods. However, freeze-drying is energy intensive and has higher costs associated with the final product, which limits the industrial application to high value products (Zhou et al. 2014). Spray-drying and freeze-drying can both produce amorphous materials by the rapid removal of solvent water from a solution (Haque and Roos 2006).

✉ Shyam S. Sablani  
ssablani@wsu.edu

✉ Hong Guo  
guohongbafs@126.com

<sup>1</sup> Beijing Academy of Food Sciences, Beijing 100068, China

<sup>2</sup> Biological Systems Engineering Department, Washington State University, Pullman, WA 99164-6120, USA

<sup>3</sup> College of Engineering, China Agricultural University, Box 194, No.17 Qinghua East Road, Beijing 100083, China

Different drying technologies may produce a different physical state and thermal transitions for amorphous materials.

Amorphous materials can be solid like a system in the glassy state or a liquid-like in the rubbery state. The glass transition involves a change in the amorphous materials from the glassy to rubbery state over a specific temperature or water content range and are dependent on the material properties (Haque and Roos 2006; Zhao et al. 2016). Above the glass transition temperature, foods are in a rubbery state and become more liquid, corresponding to a more unstable state due to the increase in the molecular mobility and a reduction in the viscosity. In contrast, below the glass transition temperature, foods in a glassy state can be considered to be very stable due to the significant decrease in the molecular mobility (Fabra et al. 2009; Zhao et al. 2015). The compounds involved in the deterioration reactions take many months or even years to diffuse over a molecular distance to react with each other in the glassy state (Slade et al. 1991; Rahman et al. 2011). Therefore, it is important to understand the thermal transition temperatures of amorphous food materials to establish the proper processing and shelf-life control procedures in the food industry.

In addition, in the food industry, liquid egg is also commonly converted into frozen egg. During both the drying and freezing processes, the formation of glassy or rubbery non-equilibrium amorphous states often occurs (Shi et al. 2012). Therefore, in order to maintain the stability of dried or frozen egg white, changes from the stable glassy state to the rubbery state should be avoided. For dried foods (low water content foods), the stability can be directly predicted from the glass line (Rahman et al. 2005; Zhao et al. 2015). However, for frozen foods (high water content foods), the maximum stability can be achieved when the freezable water transforms into ice, and the temperature is maintained below the glass transition temperature (Fabra et al. 2009; Zhang et al. 2018). The stability of frozen foods depends on the characteristic glass transition temperature of the maximal-freeze-concentration condition ( $T_g'$ ) and the characteristic end point of freezing ( $(T_m)_{\text{u}}$ ) measured using differential scanning calorimetry (DSC) (Rahman 2010). In addition, the initial freezing point ( $T_F$ ) can be used to estimate the effective molecular weight, enthalpy below freezing, and unfrozen water content (Sablani et al. 2007).

More studies have been reported on the glass transition temperatures of sugar-rich fruits compared to those of protein-water system products mainly due to the difficulty in the detection of the glass transition in protein-rich products (Sablani et al. 2007; Acevedo et al. 2006; Tolstorebrov et al. 2014; Tironi et al. 2009; Pelgrom et al. 2013). For high molecular weight protein, the change in heat capacity ( $\Delta C_p$ ) is small at a glass transition. This small change of the baseline leads to broad and indistinct transitions (Pelgrom et al. 2013; Acevedo et al. 2006). Therefore, it was difficult to measure a

clear glass transition in protein-rich foods. In addition, for high water content foods, the glass transition and ice formation is a more complicated process, and it is difficult to achieve actual maximal-freeze-concentration condition (Rahman 2004; Guizani et al. 2010; Zhao et al. 2015). In the literature, the glass transition temperatures of dried foods (low water content foods) are commonly found, but a few works report the glass transition and the maximal-freeze-concentration condition [ $(T_m)_{\text{u}}$ ,  $T_g'$ , and  $X_w$ ] in the frozen foods (high water content foods) (Sablani et al. 2010; Rahman 2010; Ogolla et al. 2019; Harnkarnsujarit et al. 2015; Tolstorebrov et al. 2014; Tironi et al. 2009). To the best of our knowledge, there is very little information available on the glass transition temperatures of egg white or whole egg (Koç et al. 2012; Rao and Labuza 2012). Koç et al. (2012) studied the effect of water on the glass transition temperature and physical properties of spray-dried whole egg powder. However, they did not analyze how to identify the step change of glass transition in the DSC curve. Rao and Labuza (2012) analyzed the glass transitions of spray-dried egg white and hydrolyzed egg white powders in the DSC curve. However, for the egg white with water content of 0.369 g water/g sample (d.b.), the glass transition temperature (66 °C) was too high. Because it is expected that such a water content sample would exhibit lower  $T_g$  than 66 °C. Therefore, further studies need to be performed to identify and determine the step change of glass transition for egg products. In addition, the thermal transitions of egg white containing freezable water (i.e., higher water contents) have not been reported.

The objective of this study was to compare the thermal transition temperatures (protein denaturation temperature, glass transition temperature, freezing point, and end point of freezing) of spray-dried and freeze-dried egg whites containing unfreezable water (i.e., lower water contents) and freezable water (i.e., higher water contents) using DSC. In addition, the water sorption isotherms of egg white samples were also established.

## Materials and Methods

### Sample Preparation

#### Spray-Dried Egg White Powders

Commercial dried egg white powders are produced by spray-drying the liquid egg white after desugarization to prevent browning due to the occurrence of the Maillard reaction (Handa et al. 2001; Sharma et al. 2012). In this study, spray-dried hen egg white powders were supplied from a local producer (Beijing Ershang Jianli Food Technology Co., Ltd., Beijing, China). Pasteurized liquid egg white was fermented using yeast to remove the glucose. After desugarization, the

liquid egg white was spray-dried and converted to egg white powder at the following operating conditions: inlet air temperature of 165–175 °C, outlet air temperature of 65–85 °C, and atomization pressure of 10 MPa.

### Freeze-Dried Egg White Powders

The freeze-dried (FD) egg white powders were prepared in our lab according to the method of Katekhong and Charoenrein (2017). There was no desugarization pretreatment before freeze-drying due to no change to a brown color through the Maillard reaction mainly because the temperature for glycosylation was low during freeze-drying the liquid egg white (Rao et al. 2013a). The liquid egg white was completely frozen at –40 °C and then placed in a freeze-dryer (Model Lyovac GT 2, Finn Aqua Santasalo-Sohlberg, Munich, Germany). The shelf temperature was set at –40 °C and drying ended at 20 °C (i.e., freeze-drying at 20 °C) under a vacuum of 15 Pa for 48 h. After freeze-drying, the samples were immediately ground by a laboratory scale grinder.

The spray-dried (SD) and FD egg white powders were stored in a desiccator over P<sub>2</sub>O<sub>5</sub> at room temperature (25 °C) for 1–3 weeks to completely dry the powders. The chemical composition of the SD and FD egg white powders was analyzed. The water, protein, fat, and ash contents of the SD and FD egg white powders were determined according to AOAC (2000). The glucose content of the egg white powders was measured by a 1260 Infinity HPLC system (Agilent Technologies, Santa Clara, CA, USA) with a G4260B evaporative light scattering detector (ELSD) as described by Djendoubi Mrad et al. (2012). An Agela Innoval NH2 (4.6 × 250 mm i.d, 5 µm particle size) was column used, and the column temperature was maintained at 40 °C.

The solubility of protein was determined according to the method used by Morr et al. (1985) with slight modifications. About 500 mg of egg white samples was added into 40 mL of 0.1 M NaCl solution with stirring in order to avoid lump formation and obtain complete sample dispersion. The pH of the dispersion was adjusted to 7.0 with 0.1 M HCl or NaOH solution. The dispersion was agitated at room temperature (25 °C) for 1 h on a magnetic stirrer. Then the dispersion was diluted to 50.0 mL with 0.1 M NaCl solution and immediately centrifuged at 10,000 r/min (17,217×g) for 30 min at 4 °C. After centrifugation, the supernatant was collected for analyses. The protein content was determined by the Kjeldahl method. The solubility was calculated by:

$$\text{Solubility (\%)} = \frac{A}{B} \times 100\% \quad (1)$$

where *A* is the content of protein in the supernatant and *B* is the total content of protein in samples.

### Scanning Electron Micrographs

The microstructures of the spray-dried and freeze-dried egg white powders were observed by scanning electron microscopy (SEM) (S-4800, Hitachi, Tokyo, Japan). Small amounts of egg white powder were sprinkled on double-sided adhesive tapes mounted on aluminum stubs. The mounted samples were then coated with gold (Haque and Roos 2006).

### Measurement and Modeling of the Water Sorption Isotherms

To obtain samples with different water activity (0.12–0.94), the SD and FD egg white powders (1.000 g) were placed in open weighing bottles, stored in airtight containers, and equilibrated for 3 to 4 weeks (until the difference between two continuous weights of the samples less than 0.001 g) using different saturated salt solutions at 25 °C (Roos and Karel 1991; Zhao et al. 2015, 2016). The salts were LiCl, CH<sub>3</sub>COOK, MgCl<sub>2</sub>·6H<sub>2</sub>O, K<sub>2</sub>CO<sub>3</sub>, Mg (NO<sub>3</sub>)<sub>2</sub>·6H<sub>2</sub>O, NaNO<sub>2</sub>, NaCl, KCl, and KNO<sub>3</sub> at equilibrium relative humidities of 12%, 23%, 33%, 44%, 52%, 61%, 75%, 85%, and 94%, respectively (Sá et al. 1999).

The water content (dry basis) of the equilibrated samples was calculated from the weight differences of the samples before and after equilibration. In addition, in order to obtain SD and FD egg white samples with water activities greater than 0.94, pre-calculated amounts of distilled water were added directly into the egg white powders in weighing bottles. The bottles were then sealed and placed in a dry desiccator at 4 °C for 24 h (Zhao et al. 2016). A small amount of thymol was placed inside the air-sealed containers for higher water activity (*a<sub>w</sub>* ≥ 0.75) to prevent microbial growth during storage.

The Guggenheim-Anderson-de Boer (GAB) equation is most commonly used to model water sorption data of food materials. The GAB model is based on the monolayer water concept and provides the monolayer water content of the materials (Rahman 1995; Zhao et al. 2015). The GAB isotherm model is shown by Eq. (2):

$$X_w = \frac{X_m C K a_w}{(1 - K a_w)(1 - K a_w + C K a_w)} \quad (2)$$

where *X<sub>w</sub>* is the water content on a dry basis; *X<sub>m</sub>* is the water content at fully occupied active sorption sites with one molecule of water, which is the safe water content for high-quality preservation of dried foods during preservation; and *C* and *K* are the GAB parameters associated with the heat of sorption of the monolayer and multilayer, respectively. The model parameters of GAB were calculated using non-linear optimization in Origin software (version 8.6).

## Determination and Modeling of the Thermal Transitions

The thermal transition temperatures (glass transition temperature, protein denaturation temperature, initial freezing point and end point of freezing) of SD and FD egg whites at different water contents were measured using DSC (Q2000, TA Instruments, New Castle, DE, USA). The DSC was calibrated for heat flow and temperature using a standard sample of indium (melting point 156.5 °C,  $\Delta H_m = 28.5$  kJ/kg) and distilled water (melting point 0.0 °C,  $\Delta H_m = 334$  kJ/kg). The egg white samples were cooled by a mechanical refrigerated cooling system. An empty sealed aluminum pan was used as a reference in each analysis. The samples (approximately 8–10 mg) were enclosed in hermetically sealed aluminum pans and then loaded onto the instrument at room temperature. Nitrogen gas at a flow rate of 50 mL/min was used as the purge gas.

### Glass Transition of Samples Containing Unfreezable Water

The egg whites with low water contents showed no formation of ice and no peak of ice melting in the DSC curve, meaning that only unfreezable water was observed in the samples (in “Results and Discussion” section). The SD and FD egg white powders containing unfreezable water ( $X_w$  range of 0.039–0.282 and 0.043–0.206 g water/g sample (w.b.) in SD and FD samples) were cooled from 20 to  $-80$  °C at 10 °C/min, equilibrated for 5 min and heated at 5 °C/min to 170 °C (Rao and Labuza 2012). TA Instruments Universal analysis software was used to analyze the data. The protein denaturation temperature ( $T_d$ ) was reported as the maximum of the endothermic denaturation peak. The  $\Delta H_d$  is the enthalpy change during the protein denaturation in the SD and FD egg white samples, and the value of  $\Delta H_d$  was estimated from the peak area of the protein denaturation as shown in Figs. 4 and 6 (Donovan et al. 1975). The glass transition temperature ( $T_g$ ) was written as onset ( $T_{gi}$ ), mid ( $T_{gm}$ ), and end points ( $T_{ge}$ ) of the glass transition as shown in Fig. 4 and Table 2.

### Glass Transition and Freezing Point of Samples Containing Freezable Water

For egg whites containing freezable water ( $X_w$  range of 0.32–0.72 and 0.31–0.73 g water/g sample (w.b.) in SD and FD samples), thermograms provided ice melting endotherms in the DSC curve (Syamaladevi et al. 2009). The glass transition and ice formation of the SD and FD egg white samples containing freezable water (i.e., higher water contents) are more complicated processes. A different scan procedure was used for the samples with higher water contents. The samples were cooled from 20 to  $-85$  °C at 5 °C/min and then equilibrated for 10 min. After equilibration, the samples were then scanned

from  $-85$  to 40 °C at 5 °C/min to initially evaluate the thermogram and to determine the end point of freezing or the start of the melting of the ice crystals ( $T_m'$ ) (Rahman 2004). To identify the maximal-freeze-concentration condition (i.e., actual  $T_g'$  and  $T_m'$ ) and to avoid the exothermic peak if present, the SD and FD egg white samples were scanned with annealing for 30 min at  $(T_m' - 1)$  °C (Guizani et al. 2010; Zhao et al. 2015). The annealing procedure was as follows: samples were cooled from 20 to  $-85$  °C at 5 °C/min, heated at 5 °C/min up to  $(T_m' - 1)$  °C, and equilibrated for 30 min. After annealing, the egg white samples were cooled from  $(T_m' - 1)$  °C to  $-85$  °C at 5 °C/min. Finally, the samples were reheated from  $-85$  to 40 °C at 5 °C/min. Similar scan procedures were also used by Rahman et al. (2010), Sablani et al. (2007), and Shi et al. (2009) for protein foods containing freezable water.

The initial freezing point ( $T_F$ ) was considered to be the temperature at the point of maximum slope of the endothermic peak (Syamaladevi et al. 2009). The end point of freezing ( $T_m'$ ) of the egg white samples was reported as the point at which the baseline intersected with the left side of the endotherm. The  $\Delta H_m$  is the enthalpy change during the melting of ice in the SD and FD egg white samples, and the value of  $\Delta H_m$  was estimated from the area of the melting endotherm as shown in Fig. 7 (Rahman 2004). In addition, the  $T_m'$  at unfreezable water content ( $X_w'$ ) was considered the characteristic end point of freezing of the ultimate maximal-freeze-concentration condition ( $T_m'_{u}$ ).

The changes of the glass transition temperature in foods and biological materials with water content are commonly modeled using the Gordon-Taylor (GT) equation. The GT equation is shown by (Gordon and Taylor 1952):

$$T_{gm} = \frac{X_s(T_{gs}) + kX_w(T_{gw})}{X_s + kX_w} \quad (3)$$

where  $X_s$  and  $X_w$  are the mass fraction of solids and water (wet basis), respectively;  $T_{gm}$ ,  $T_{gs}$ , and  $T_{gw}$  are the glass transition temperatures of the mixture, solids, and water, respectively.  $T_{gw} = -135$  °C;  $k$  is the Gordon-Taylor parameter (Zhao et al. 2015, 2016). The model parameters of the GT equation were estimated using non-linear optimization in the Origin software (version 8.6).

The theoretical Clausius-Clapeyron equation was used to fit the freezing curve of the SD and FD egg white samples with different water contents. The Clausius-Clapeyron equation is provided as Eq. (4) (Rahman 1995):

$$\Delta = -\frac{\beta}{\lambda_w} \ln \left[ \frac{1-X_s}{1-X_s + EX_s} \right] \quad (4)$$

where  $\Delta$  is the freezing point depression ( $T_w - T_F$ );  $T_F$  is the initial freezing point of the samples (°C);  $T_w$  is the freezing point of water (°C);  $\beta$  is the molar freezing point constant of water (1860 kg K/kg mol);  $\lambda_w$  is the molecular mass of water;

$X_s$  is the solids mass fraction (wet basis); and  $E$  is the molecular mass ratio of water to solids ( $\lambda_w/\lambda_s$ ). The model parameter  $E$  of Eq. (4) was estimated using non-linear optimization in Origin software (version 8.6).

### Statistical Analysis

All samples were measured in three replicates. The results were written as mean  $\pm$  standard deviation (SD). The data were analyzed by one-way analysis of variance (ANOVA). The statistical significance of results was determined using SPSS 17.0 software (SPSS, Chicago, IL, USA). The significant difference between average values was assessed using Duncan's test at a significance level of  $P < 0.05$ .

The goodness of fit of each model was evaluated using the correlation coefficient ( $R^2$ ), root mean square error (RMSE), and reduced chi-square ( $\chi^2$ ) which are given by:

$$\text{RMSE} = \sqrt{\frac{\sum_{i=1}^N (X_{\text{exp},i} - X_{\text{pred},i})^2}{N}} \quad (5)$$

$$\chi^2 = \frac{\sum_{i=1}^N (X_{\text{exp},i} - X_{\text{pred},i})^2}{N-n} \quad (6)$$

where  $X_{\text{exp},i}$  and  $X_{\text{pred},i}$  are the  $i$ th experimental and the  $i$ th predicted values, respectively.  $N$  and  $n$  are the number of observations and the number of constants in each model, respectively. A model is considered as good when  $R^2$  is high, RMSE is low, and  $\chi^2$  is reduced (Singh and Mehta 2008; Wang and Zhou 2013).

## Results and Discussion

### Microstructure of the Spray-Dried and Freeze-Dried Egg White Powders

The microstructures of the SD and FD egg white powders were observed by scanning electron microscopy (SEM) as shown in Fig. 1a and b. The results showed that the SD amorphous egg white had round-shaped particles with a smooth surface or with some dents. Alternatively, the FD amorphous egg white resembled broken glass or showed a flake-like structure. Similar microstructures were observed for the SD and FD amorphous lactose and lactose/protein mixtures (Haque and Roos 2006) and for the SD and FD egg white protein hydrolysates (Chen et al. 2012). The different microstructures of the SD and FD amorphous egg white were mainly due to atomization during the spray-drying, which resulted in smaller atomized droplets with spherical shape. However, the freeze-drying method lacked the forces for splitting the

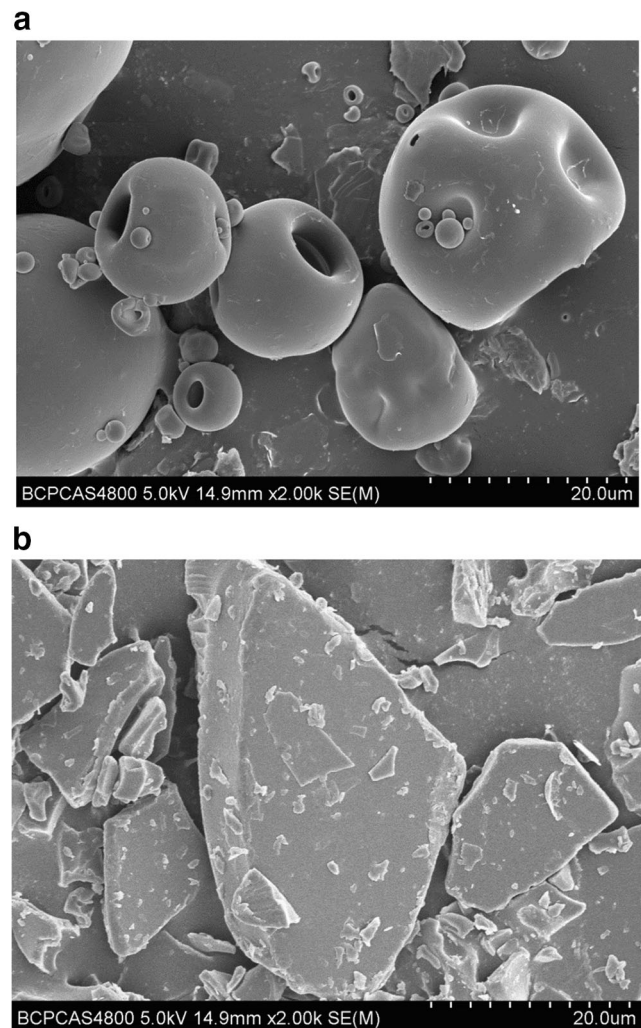


**Fig. 1** Scanning electron micrographs of spray-dried (a) and freeze-dried egg white powders (b).  $\times 2000$  magnification

frozen liquid into droplets during the evaporation process, which may lead to flake-like microstructures and larger particles of the FD egg white powders (Chen et al. 2012). In this study, the results indicate that different drying methods can cause different microstructures of the SD and FD amorphous egg whites.

### Sorption Isotherms of Spray-Dried and Freeze-Dried Egg White Powders

The water, protein, fat, ash, and glucose contents of the SD egg white powders were 8.34, 71.0, 0.212, 3.60, and 0% (wet basis), respectively. In addition, the water, protein, fat, ash, and glucose contents of the FD samples were 8.02, 70.9, 0.110, 2.93, and 1.20% (wet basis), respectively. The fat and ash contents of the SD egg white powders were greater than those of the FD samples, and the other contents of both samples were similar. There was no glucose detected in the SD egg white powders, mainly because glucose was removed

from the liquid egg white to prevent browning before spray-drying. While, in the FD egg white powders, there was no desugarization pre-treatment before freeze-drying. In addition, non-covalently bound glucose can be detected in the FD egg white powders mainly because the temperature for glycosylation through the Maillard reaction was low ( $-40\text{--}20\text{ }^{\circ}\text{C}$ ) during freeze-drying (Rao et al. 2013a).

The sorption isotherms of the SD and FD egg whites at  $25\text{ }^{\circ}\text{C}$  are shown in Fig. 2. There was no significant difference ( $P > 0.05$ ) between the SD and FD isotherms. However, Haque and Roos (2006) reported that the FD lactose and lactose/protein mixtures absorbed higher amounts of water than the SD samples at all corresponding relative water vapor pressure (RVP), as the SD samples may have fewer hydrogen bonding sites available for water molecule sorption than the FD samples due to the different drying methods. In this study, the SD and FD egg white samples absorbed similar amounts of water at all water activities. As expected, the equilibrium water content increased with increasing water activity. Both the SD and FD egg white powders tended to absorb small amounts of water at low and intermediate water activities ( $a_w < 0.52$ ), whereas at high water activities ( $a_w > 0.52$ ), water rapidly increased with water activity due to possibly more active sites (Zhao et al. 2015). The sorption isotherms of two products followed type II (sigmoidal curve) behavior, typical of protein-rich products. This water sorption behavior was similar to sorption isotherms of other egg white powders (Rao and Labuza 2012) and whole egg powders (Koç et al. 2012).

The values of the parameters for the GAB model of SD and FD egg white powders are shown in Table 1. The GAB model fit very well with the experimental data of both samples according to the higher values of  $R^2$  and lower values of  $\chi^2$  and RMSE. The monolayer water contents ( $X_m$ ) of SD and FD egg white powders were similar. According to the water activity concept, food products were most stable at its  $X_m$  or

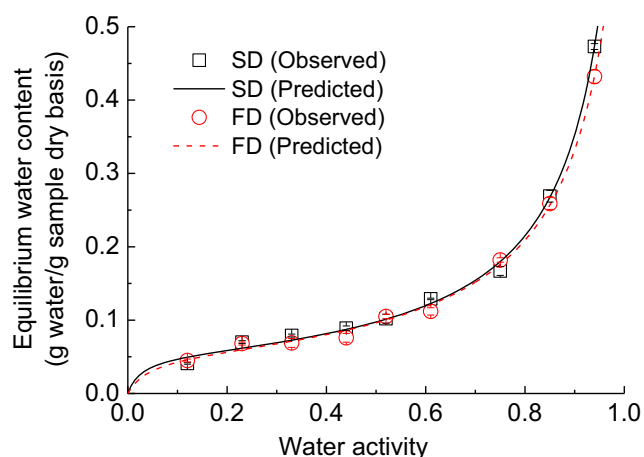


**Fig. 2** Sorption isotherms of spray-dried and freeze-dried egg white powders at  $25\text{ }^{\circ}\text{C}$

monolayer water activity (Rahman 2009; Zhao et al. 2015). Therefore, at a given temperature, the safest water activity level is that corresponding to  $X_m$  (Rahman 2009).  $X_m$  has a direct influence on lipid oxidation, enzymatic activity, non-enzymatic browning, flavor preservation, and product structure of egg products during storage (Koç et al. 2012).  $X_m$  obtained for other egg powders are shown in Table 1. The multilayer factor ( $K$ ) was similar for the SD and FD samples, while the surface heat constant ( $C$ ) of the SD egg white powders was greater than that of the FD egg white powders, implying that the water molecules were more tightly bound in the SD samples (Rao and Labuza 2012).

## Thermal Transitions of Egg White Containing Unfreezable Water

### Thermal Transitions of Spray-Dried Egg White Containing Unfreezable Water

The thermal transition temperatures of the SD egg whites containing unfreezable water (0.039–0.282 g water/g sample (w.b.)) as a function of water content are present in Table 2. The thermograms of the SD egg whites with water contents ranging from 0.039 to 0.212 g water/g sample (w.b.) ( $a_w$  of 0.12–0.85) are shown in Fig. 3. The thermograms of the egg whites with low water contents ( $X_w \leq$  unfreezable water content of 0.283 g water/g samples (w.b.) in Eq. (7)) exhibited no formation of ice and no peak of ice melting in the DSC thermogram. Similar thermograms were also observed by Rahman et al. (2005), Syamaladevi et al. (2009), Zhao et al. (2015), and Zhao et al. (2016).

The SD egg white samples in the middle  $a_w$  range (0.44–0.75) with water contents ranging from 0.082 to 0.143 g water/g sample (w.b.) that showed two denaturation peaks. The location of peak 1 resembled the step change of the glass transition, which, according to the literature, can be attributed to the location of the denaturation peak of ovotransferrin (Donovan et al. 1975; Rao and Labuza 2012) because the  $T_d$  of ovotransferrin in water or buffer is  $61.0\text{ }^{\circ}\text{C}$  (Rao and Labuza 2012). In this study, the values of  $T_d$  of ovotransferrin ranging from  $52.8$  to  $67.9\text{ }^{\circ}\text{C}$  were close to  $61.0\text{ }^{\circ}\text{C}$  in the solution state. Some studies have also reported that peak 2 can be attributed to the denaturation of ovalbumin. The  $T_d$  of ovalbumin in water or buffer is  $84.0\text{ }^{\circ}\text{C}$  (Donovan et al. 1975; Rao and Labuza 2012). The  $T_{d1}$  of ovotransferrin decreased from  $67.9$  to  $52.8\text{ }^{\circ}\text{C}$  when the water content increased from 0.082 to 0.143 g water/g sample (w.b.). In addition, the  $T_{d2}$  of ovalbumin decreased from  $136.0$  to  $87.8\text{ }^{\circ}\text{C}$  when the water content increased from 0.039 to 0.212 g water/g sample (w.b.). This result indicates that water content (0.039–0.212 g water/g sample (w.b.)) showed a strong influence on the  $T_{d2}$  of ovalbumin.

**Table 1** GAB fitting for sorption experimental data of egg white

| GAB parameters         | Spray-dried egg white <sup>a</sup> | Spray-dried egg yolk <sup>b</sup> | Spray-dried whole egg <sup>c</sup> | Spray-dried egg white <sup>d</sup> | Freeze-dried egg white <sup>d</sup> |
|------------------------|------------------------------------|-----------------------------------|------------------------------------|------------------------------------|-------------------------------------|
| $X_m$ /(g/g dry basis) | 0.062                              | 0.023                             | 0.145                              | 0.053                              | 0.054                               |
| $C$                    | 32.5                               | 11.5                              | 1.661                              | 37.7                               | 24.9                                |
| $K$                    | 0.99                               | 0.98                              | 0.810                              | 0.945                              | 0.932                               |
| $R^2_{GAB}$            | –                                  | –                                 | 0.997                              | 0.996                              | 0.997                               |
| MAPE                   | 4.2                                | 8.3                               | –                                  | –                                  | –                                   |
| RMSE                   | –                                  | –                                 | –                                  | $6.572 \times 10^{-3}$             | $6.072 \times 10^{-3}$              |
| $\chi^2$               | –                                  | –                                 | –                                  | $6.515 \times 10^{-5}$             | $6.495 \times 10^{-5}$              |

<sup>a</sup> Rao and Labuza (2012)

<sup>b</sup> Rao et al. (2013b)

<sup>c</sup> Koç et al. (2012)

<sup>d</sup> Current work

$R^2$  correlation coefficient, MAPE mean absolute percentage error, RMSE root mean square error,  $\chi^2$  reduced chi-square, – No data

The glass transition temperature ( $T_g$ ) of the SD egg white powder was observed at water content from 0.039 to 0.093 g water/g sample (w.b.) ( $a_w$  of 0.12–0.52) as shown in Table 2 and Fig. 3. However, in the range of middle  $a_w$  from 0.61 to 0.85 ( $X_w$  of 0.114–0.212 g water/g sample (w.b.)), the  $T_g$  of SD samples was not detected, possibly due to the overlapping ovotransferrin denaturation peak. To increase the sensitivity of the thermal analysis, modulated differential scanning calorimetry (MDSC) was also used to trace the glass transition temperatures in these samples of  $X_w$  from 0.114 to 0.212 g

water/g sample (w.b.) (data not shown). The results also showed no clear step change in the reversible heat flow. Similar results were reported by Rao and Labuza (2012), in which there was no  $T_g$  of dried egg whites in the range of middle  $a_w$  from 0.43 to 0.76. In this study, Fig. 4 shows two denaturation peaks and one glass transition temperature of the SD egg whites at a water content of 0.082 g water/g sample (w.b.). The onset  $T_{gi}$  and final  $T_{ge}$  points of transitions were obtained by extrapolating the side and baselines as shown in Fig. 4. In addition, transitions were observed in the range of

**Table 2** Thermal transitions of spray-dried egg white containing unfreezable water

| $X_w$ (g/g (w.b.)) | Ovotransferrin (peak 1) |                              |                           |                           |                           | Ovalbumin (peak 2) |                              |
|--------------------|-------------------------|------------------------------|---------------------------|---------------------------|---------------------------|--------------------|------------------------------|
|                    | $T_{d1}$ (°C)           | $\Delta H_{d1}$ (J/g (d.b.)) | $T_{gi}$ (°C)             | $T_{gm}$ (°C)             | $T_{ge}$ (°C)             | $T_{d2}$ (°C)      | $\Delta H_{d2}$ (J/g (d.b.)) |
| 0.039              | –                       | –                            | 112.0 ± 2.8a              | 116.0 ± 3.3a              | 116.7 ± 2.8a              | 136.0 ± 2.4a       | 5.56 ± 0.18b                 |
| 0.065              | –                       | –                            | 100.7 ± 4.6b              | 103.6 ± 4.4b              | 105.1 ± 4.0b              | 127.5 ± 3.6b       | 2.37 ± 0.33e                 |
| 0.073              | –                       | –                            | 94.8 ± 3.6c               | 96.0 ± 1.7c               | 99.0 ± 1.2c               | 123.1 ± 1.8c       | 3.96 ± 0.23d                 |
| 0.082              | 67.9 ± 2.4a             | 0.686 ± 0.077b               | 87.5 ± 2.0d               | 90.7 ± 3.3d               | 94.4 ± 0.9d               | 118.8 ± 0.5d       | 4.72 ± 0.39c                 |
| 0.093              | 67.6 ± 0.6a             | 0.278 ± 0.029c               | 85.3 ± 1.5d               | 88.4 ± 0.3d               | 91.7 ± 0.1e               | 117.4 ± 0.1d       | 7.38 ± 0.92a                 |
| 0.114              | 59.9 ± 1.2b             | 1.042 ± 0.043a               | –                         | –                         | –                         | 106.1 ± 0.3e       | 4.11 ± 0.24d                 |
| 0.143              | 52.8 ± 2.4c             | 0.258 ± 0.037c               | –                         | –                         | –                         | 99.4 ± 2.0f        | 5.42 ± 0.78b                 |
| 0.212              | –                       | –                            | –                         | –                         | –                         | 87.8 ± 0.9gh       | 5.95 ± 0.81b                 |
| 0.238              | –                       | –                            | 65.3 ± 0.6e <sup>x</sup>  | 70.2 ± 0.4e <sup>x</sup>  | 74.0 ± 0.2f <sup>x</sup>  | 87.1 ± 1.0h        | 1.44 ± 0.14f                 |
| 0.257              | –                       | –                            | 65.1 ± 1.2e <sup>x</sup>  | 68.5 ± 1.3ef <sup>x</sup> | 72.0 ± 1.5fg <sup>x</sup> | 87.6 ± 2.3gh       | 2.01 ± 0.16ef                |
| 0.269              | –                       | –                            | 63.6 ± 0.8ef <sup>x</sup> | 67.5 ± 0.6ef <sup>x</sup> | 71.2 ± 0.7g <sup>x</sup>  | 87.3 ± 1.6gh       | 1.85 ± 0.15ef                |
| 0.282              | –                       | –                            | 61.8 ± 1.1f <sup>x</sup>  | 66.2 ± 1.2f <sup>x</sup>  | 70.2 ± 1.6g <sup>x</sup>  | 89.5 ± 1.3g        | 1.77 ± 0.14f                 |

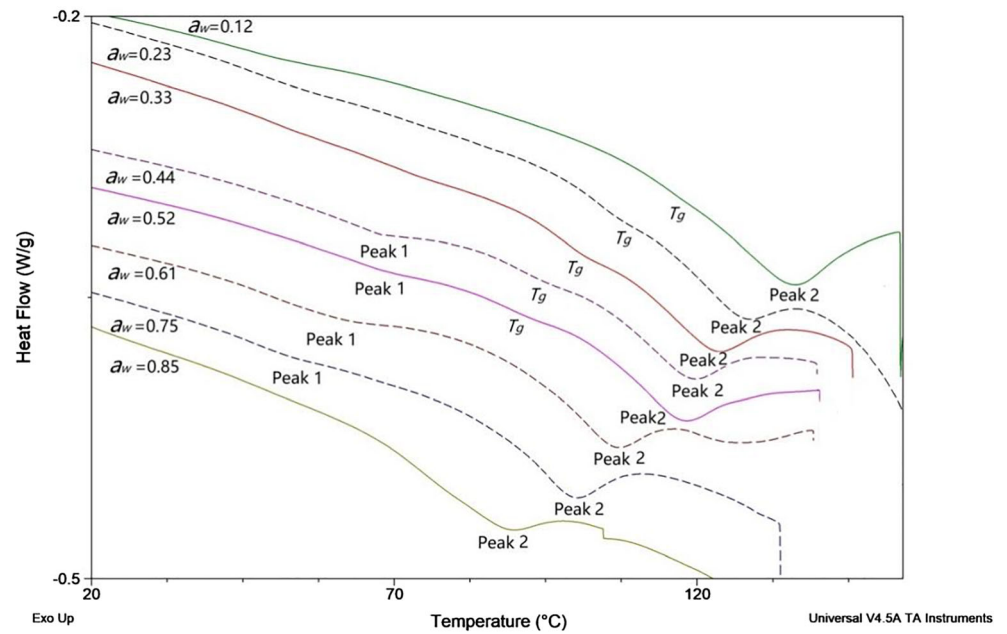
Each value is written as mean ± SD ( $n = 3$ )

–: Not detectable

Different small letters (a–h) within the same column represent significant difference ( $P < 0.05$ )

<sup>x</sup> The shifts resemble the glass transition but these data are not considered glass transition temperatures

**Fig. 3** DSC thermograms of spray-dried egg white containing unfreezable water ( $a_w$  of 0.12–0.85,  $X_w$  of 0.039–0.212 g water/g sample (w.b.))

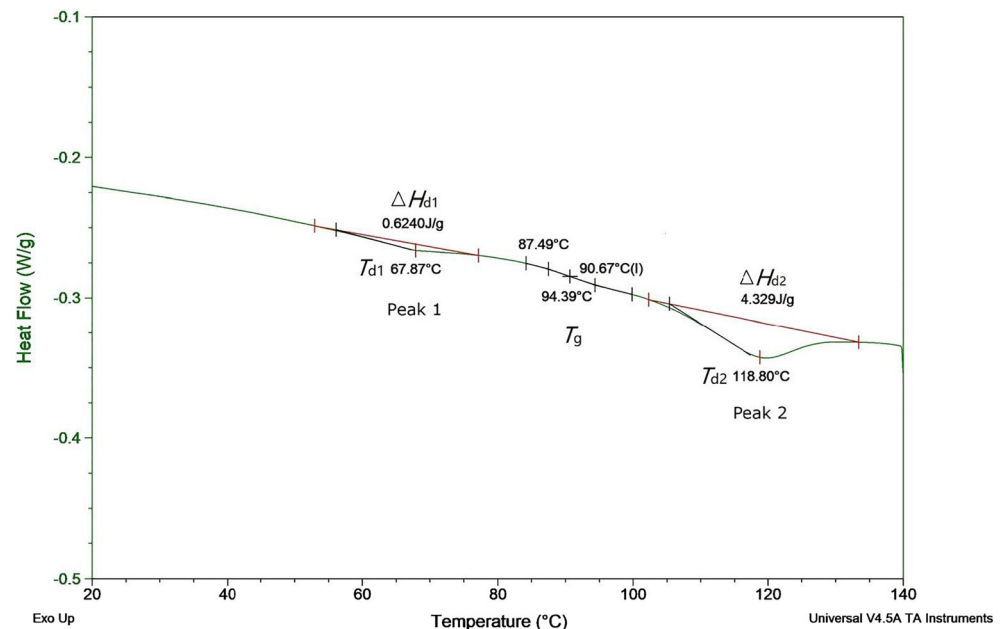


$X_w$  from 0.238 to 0.282 ( $X_w \leq$  unfreezable water content), as shown in Table 2. However, the increasing water content had little influence on the change in the glass transition temperature, which indicates that the plasticization effects of water on the protein were very small. Moreover, these glass transition temperatures were too high for the samples with  $X_w$  from 0.238 to 0.282 g water/g sample (w.b.), and thus, they were not reasonable. Rao and Labuza (2012) reported that  $T_g$  was 66 °C for the spray-dried egg white with  $X_w$  of 0.369 g water/g sample (d.b.). Koç et al. (2012) found that  $T_g$  ranged from 90.5 to 71.3 °C for the spray-dried whole egg with  $X_w$  from 0.240 to 0.354 g water/g sample (d.b.). However, it is expected that

such water contents egg white and whole egg samples would show lower  $T_g$  than 66 and 71.3 °C, respectively. Therefore, these shifts could not be considered glass transition temperatures and could be due to some other relaxation processes. Sablani et al. (2007) observed similar phenomenon for protein in king fish muscle.

The glass transition temperatures of food components (carbohydrate or protein) depend mainly on the quantity of water, and the composition and molecular weight of the solutes present in the food. In this study,  $T_{gi}$  was taken as the glass transition temperature of the SD samples, i.e., the point where samples remained completely in the glass form (Guizani

**Fig. 4** Thermal transition temperatures of spray-dried egg white powders with 0.082 g water/g sample (w.b.) ( $a_w$  of 0.44)



et al. 2010; Rahman et al. 2005; Zhao et al. 2016). When the water content of the SD egg white increased from 0.039 to 0.093 g water/g sample (w.b.), the  $T_{gi}$  decreased from 112.0 to 85.3 °C (in Table 2). The expected decrease in the  $T_g$  of SD egg whites with increasing water content was mainly due to the plasticization effect of water on the amorphous constituents of the matrix (Rahman et al. 2005; Zhao et al. 2015; Harnkarnsujarit et al. 2015). Water is a strong plasticizer and has a low molecular weight and glass transition temperature (−135 °C), which can increase the free volume between the molecules of the amorphous matrix. More studies on the glass transition temperatures of protein-rich foods have been reported for fishery products. The  $T_g$  of the SD egg white was greater than that of fish at the same water content (Tolstorebrov et al. 2014; Shi et al. 2009).

The change in the glass transition temperatures with solid content (i.e., glass transition curve) was predicted by fitting the Gordon-Taylor (GT) equation in Fig. 5. The model constants  $T_{gs}$  and  $k$  were calculated as 135.3 °C and 2.255, respectively. Good agreement between the experimental and predicted glass transition temperature values was obtained based on the higher values of  $R^2$  (0.968) and lower values of  $\chi^2$  (3.780) and RMSE (1.511). The  $k$  value can be used to estimate the plasticization effect of water, which means the strength of the interaction between water and food solids. Higher values show a greater plasticization effect of water on the food solids (Sablani et al. 2010; Zhao et al. 2016, 2018). The  $k$  value obtained for the SD egg white powders was similar to that of other protein foods, including 2.89 for tuna meat (Rahman et al. 2003), 5.01 for horse mackerel (Shi et al. 2009), and 5.0 for surimi-trehalose mixture (Ohkuma et al. 2008). The variation may be due to the differences in chemical composition of the foods and methods used for thermal transition analysis of the samples.

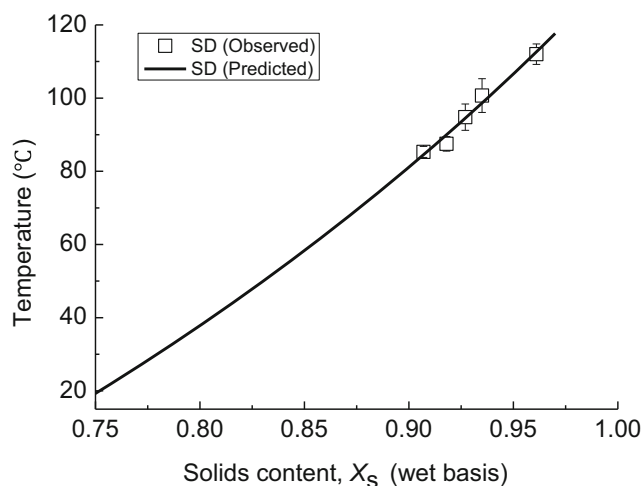


**Fig. 5**  $T_g$ - $X_s$  relationship of spray-dried egg white with different solids content

### Thermal Transitions of the Freeze-Dried Egg White Containing Unfreezable Water

As shown in Table 3, the FD egg whites with water contents ranging from 0.043 to 0.101 g water/g sample (w.b.) ( $a_w$  of 0.12–0.61) also showed denaturation peaks ( $T_{d1}$  and  $T_{d2}$ ). The changing trend in the  $T_{d2}$  of ovalbumin in the FD egg whites with water content (0.065–0.206 g water/g sample (w.b.)) were similar to that in the SD egg white samples. As the water content increased, the  $T_{d1}$  of ovotransferrin in the FD egg white exhibited smaller changes and was close to the  $T_d$  of ovotransferrin (61.0 °C) in the solution state. In the range of  $X_w$  from 0.043 to 0.101 g water/g sample (w.b.), the glass transition of the FD egg white was not detected. MDSC was also used to measure the glass transition temperatures in these samples of  $X_w$  from 0.043 to 0.101 g water/g sample (w.b.) (data not shown). The results also showed no clear detectable glass transition in the reversible heat flow. Similarly, Acevedo et al. (2006) noted difficulty in measuring the glass transition for freeze-dried chicken muscle using DSC. They explained that the high amount of insoluble proteins and low amount of sugars caused the difficulty in determination of  $T_g$ . In addition, in the range of  $X_w$  of 0.154 to 0.206 g water/g sample (w.b.) ( $a_w$  of 0.75 and 0.85), the transition shifts were similar to the step changes of the glass transitions shown in Fig. 6. However, these shifts may not be considered glass transition temperatures and could be due to other relaxation processes. This observation is consistent with the results of the SD egg white samples with high water content (0.238–0.282 g water/g sample (w.b.)).

There were some reasons to explain why the thermal transition temperatures of FD egg white were different from those of the SD egg white. In the literature, Hashimoto et al. (2004) found that freeze-dried fish muscle without heat-treatment before drying (non-denatured) did not have clear glass transition due to the relatively small  $\Delta C_p$  in the DSC curve, while boiled and freeze-dried sample (heat-denatured) exhibited clear glass transition because  $\Delta C_p$  was larger than that of non-denatured sample. Sochava and Smirnova (1993) also observed that the glass transitions of non-denatured globular proteins were difficult to trace, while the glass transitions of heat-denatured samples were easy to trace. Their results indicate that denaturation increased the heat capacity at glass transition. In this study, the residual denaturation enthalpies of SD egg whites ( $\Delta H_{d1}$  and  $\Delta H_{d2}$ ) were less than those of FD samples in Tables 2 and 3. This result indicates that the denaturation level of egg white proteins (ovotransferrin and ovalbumin) for SD samples was higher than that of FD samples mainly due to thermal treatment during the spray-drying, which could lead to larger  $\Delta C_p$  at a glass transition of SD samples compared to FD samples in the DSC curve. Therefore,  $T_g$  of SD egg white was more easily detected than that of the FD egg white containing unfreezable water. The results for globular proteins,

**Table 3** Thermal transitions of freeze-dried egg white containing unfreezeable water

| $X_w$ (g/g (w.b.)) | Ovotransferrin (peak 1) |                              |                          | Ovalbumin (peak 2)       |                          |                |                              |
|--------------------|-------------------------|------------------------------|--------------------------|--------------------------|--------------------------|----------------|------------------------------|
|                    | $T_{d1}$ (°C)           | $\Delta H_{d1}$ (J/g (d.b.)) | $T_{gi}$ (°C)            | $T_{gm}$ (°C)            | $T_{ge}$ (°C)            | $T_{d2}$ (°C)  | $\Delta H_{d2}$ (J/g (d.b.)) |
| 0.043              | 62.9 ± 1.5ab            | 1.08 ± 0.33bc                | —                        | —                        | —                        | 103.4 ± 2.4bc  | 13.9 ± 1.5a                  |
| 0.064              | 62.8 ± 2.3ab            | 1.30 ± 0.46ab                | —                        | —                        | —                        | 104.0 ± 1.8abc | 11.9 ± 1.3ab                 |
| 0.065              | 64.3 ± 2.8a             | 1.47 ± 0.12a                 | —                        | —                        | —                        | 105.5 ± 0.6a   | 11.7 ± 1.2b                  |
| 0.071              | 61.2 ± 2.2b             | 1.17 ± 0.28abc               | —                        | —                        | —                        | 104.6 ± 0.6ab  | 12.5 ± 1.1ab                 |
| 0.095              | 61.1 ± 0.4b             | 1.06 ± 0.09bc                | —                        | —                        | —                        | 102.0 ± 1.3c   | 13.7 ± 3.3a                  |
| 0.101              | 61.0 ± 2.3b             | 0.901 ± 0.091c               | —                        | —                        | —                        | 99.8 ± 2.1d    | 9.13 ± 0.84c                 |
| 0.154              | —                       | —                            | 77.2 ± 0.2a <sup>x</sup> | 80.9 ± 1.1a <sup>x</sup> | 83.5 ± 1.1a <sup>x</sup> | 96.0 ± 1.5e    | 2.78 ± 0.12d                 |
| 0.206              | —                       | —                            | 71.8 ± 1.9b <sup>x</sup> | 76.0 ± 1.1b <sup>x</sup> | 78.4 ± 0.7b <sup>x</sup> | 91.5 ± 1.2f    | 4.03 ± 0.77d                 |

Each value is written as mean ± SD ( $n = 3$ )

—: Not detectable

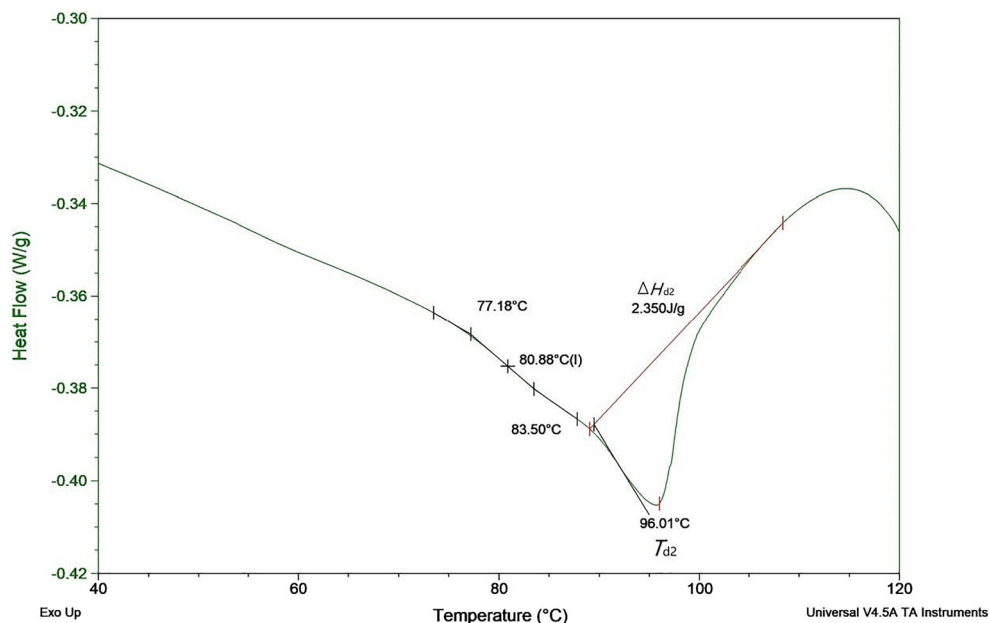
Different small letters (a–f) within the same column represent significant difference ( $P < 0.05$ )

<sup>x</sup> The shifts resemble the glass transition but these data are not considered glass transition temperatures

fish muscle, and our result indicate that the step change of glass transition is related to the heat denaturation of its proteins, and thus the heat denaturation of proteins affects the detection of the glass transition in the DSC curve. In addition, the spray-drying and freeze-drying processes may lead to the denaturation and aggregation of egg white proteins. The denaturation followed by aggregation of protein can influence their solubility/hydration properties (Harnkarnsujarit et al. 2015; Tironi et al. 2007; Katekhong and Charoenrein 2017). The solubility of SD egg white powders (73.6%) was different from that of the FD egg white powders (82.7%). Besides the protein aggregates, many other factors also affect the protein solubility, such as pH, ionic strength, pressure, temperature,

and mechanical disruption forces (Ferreira Machado et al. 2007). The different solubility was related to the different water-binding capacity of proteins between SD and FD egg whites. The different water-binding capacity of proteins may cause the different glass-forming systems (hydrated proteins), and thus leading to the different thermal transitions between SD and FD egg whites. Tironi et al. (2009) observed that the glass transition temperatures increased after high-pressure treatment for sea bass muscle. They analyzed that the change would be associated with denaturation and aggregation of fish muscle proteins. Further study is required to determine the reason for the different thermal transitions of SD and FD egg whites.

**Fig. 6** Thermal transition temperatures of freeze-dried egg white with 0.154 g water/g sample (w.b)

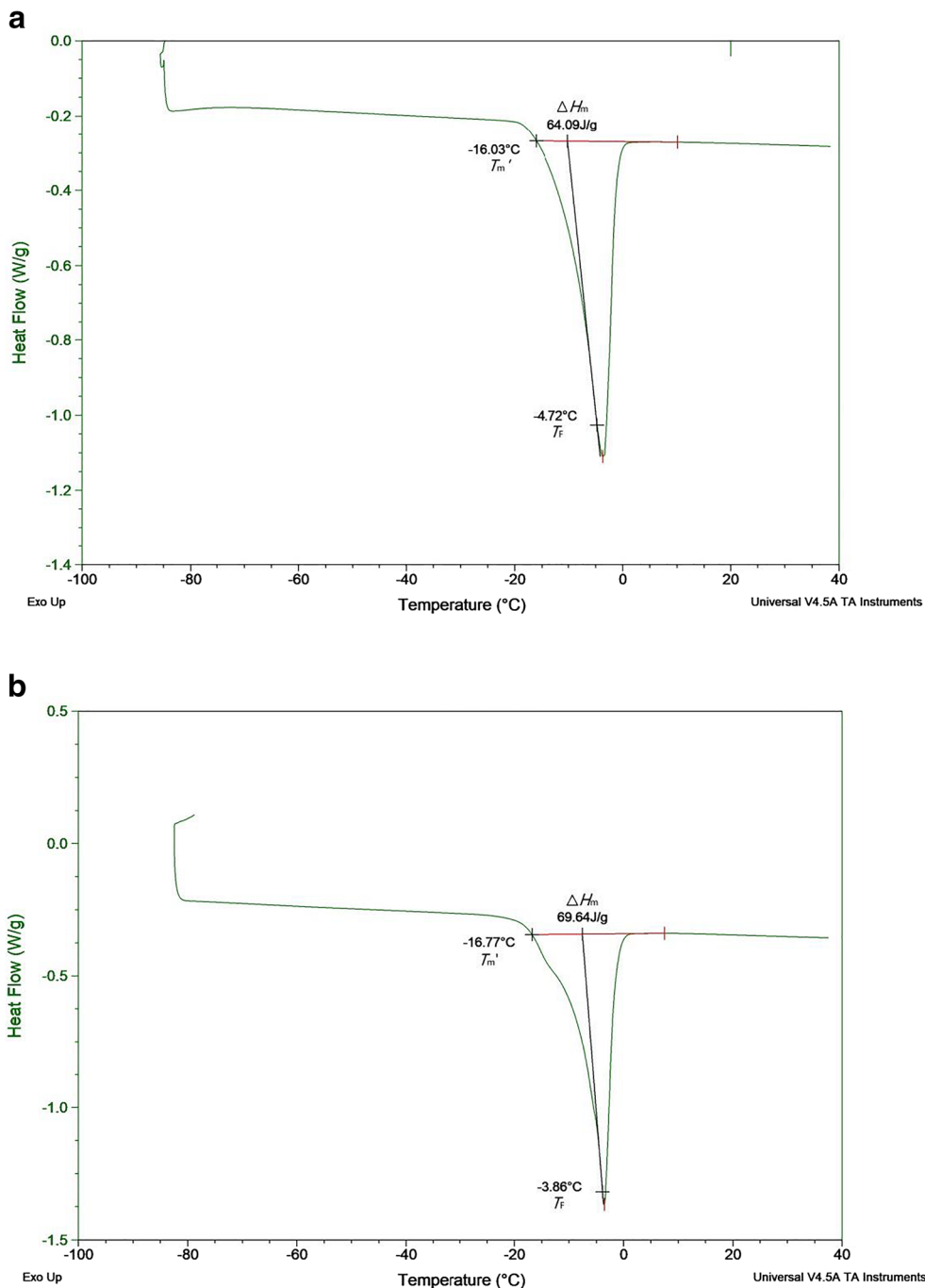


### Thermal Transitions of Egg White Containing Freezable Water

Figure 7a and b shows typical DSC thermograms for the annealed SD and FD egg whites with high water contents (containing freezable water) of 0.44 and 0.45 g water/g sample (w.b.), respectively. The values of the initial freezing points ( $T_F$ ), end point of freezing ( $T_m'$ ) and enthalpy of ice melting ( $\Delta H_m$ ) for the SD egg whites were  $-4.72^\circ\text{C}$ ,  $-16.0^\circ\text{C}$ , and  $64.1\text{ J/g}$ , respectively (Fig. 7a). The  $T_F$ ,  $T_m'$ , and  $\Delta H_m$  for the FD egg white were

$-3.86^\circ\text{C}$ ,  $-16.8^\circ\text{C}$ , and  $69.6\text{ J/g}$ , respectively (Fig. 7b). The glass transition temperatures in the freeze-concentrated matrix ( $T_g'$ ) were not detected in all of the SD and FD samples containing freezable water, and only the peak of ice melting was observed. This phenomenon may be due to the lower  $\Delta C_p$  values at a glass transition in heat flow for protein foods; as a result, these shifts of the baselines were difficult to obtain (Acevedo et al. 2006). This result indicates that the transition shifts were outside the detectable limits of the DSC. Sablani et al. (2007) also faced difficulty in tracing the glass transition temperatures of king fish

**Fig. 7** Typical DSC thermogram of spray-dried egg white containing freezable water (0.44 g water/g sample (w.b.)) (a) and freeze-dried egg white containing freezable water (0.45 g water/g sample (w.b.)) (b)



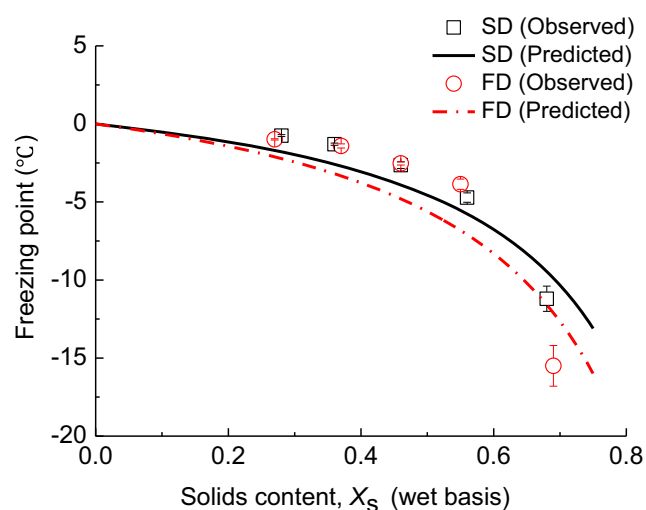
whole muscle by DSC. Ohkuma et al. (2008) reported that no apparent glass transitions were detected in frozen surimi-sugar mixtures containing sugar at concentrations of less than 30.0% (d.b.). Sablani et al. (2007) explained that for a complex food system, it was difficult to obtain a clear glass transition with thermal analysis due to interference of other physical and chemical changes, or the complexity of the structure affected the determination of the glass transition.

Figure 8 shows the change in the freezing point with solids content (i.e., freezing curve). In Fig. 8 and Table 4, the  $T_F$  decreased from  $-0.75$  to  $-11.2$  °C when the solids content ( $X_s$ ) of the SD egg white increased from 0.28 to 0.68 g solids/g sample (w.b.). The  $T_F$  decreased from  $-0.99$  to  $-15.5$  °C when the  $X_s$  of the FD egg white increased from 0.27 to 0.69 g solids/g sample (w.b.). The  $T_F$  is closely correlated with the concentration of soluble solids present in the aqueous phase. Shi et al. (2015) also showed that the  $T_F$  of *Penaeus vannamei* meat decreased with increasing solids content.

The  $\Delta H_m$  of the SD egg white decreased from 182.6 to 16.4 J/g when the water content decreased from 0.72 to 0.32 g water/g sample (w.b.) (Table 4). The  $\Delta H_m$  was plotted against the water content as shown in Fig. 9, and the unfreezable water content was calculated when the  $\Delta H_m$  was equal to zero. A linear relationship between the  $\Delta H_m$  and the water content for SD egg white is shown in Eq. (7):

$$\Delta H_m = 412.8X_w - 116.7 \quad (7)$$

The content of unfreezable water in the SD egg white was calculated from Eq. (7) as 0.283 g/g (w.b.), and the  $R^2$  was 0.999. Similarly, the content of unfreezable water in the FD egg white was calculated as 0.228 g/g (w.b.) from Eq. (8), using the same method of extrapolated  $\Delta H_m$  values, and the  $R^2$  was 0.950.



**Fig. 8** Plot of freezing point as a function of solids content in spray-dried and freeze-dried egg white

$$\Delta H_m = 302.3X_w - 68.8 \quad (8)$$

The content of unfreezable water in the SD egg white was greater than that of the FD egg white, which may be because the surface heat constant ( $C$ ) of the SD egg white powders was greater than that of the FD egg white powders in the GAB model, indicating that the water molecule in the SD samples was more tightly bound (in Table 1), and thus, higher unfreezable water was observed in the SD sample at the maximal-freeze-concentration condition. The unfreezable water contents reported for other protein foods were 0.26 g/g (w.b.) for bovine gelatin (Rahman et al. 2010), 0.320 g/g (w.b.) for abalone (Sablani et al. 2004), 0.312 g/g (w.b.) for king fish muscle (Sablani et al. 2007), 0.262 g/g (w.b.) for *P. vannamei* meat (Shi et al. 2015), 0.244 g/g (w.b.) for Atlantic cod muscles (Tolstorebrov et al. 2014), and 0.214 g/g (w.b.) for horse mackerel muscle (Shi et al. 2009). The unfreezable water is the water remaining unfrozen even at very low temperatures, and it does not undergo crystallization due to the extremely high viscosity. The unfreezable water contains both un-crystallized free water and bound water attached to the solid matrix (Rahman 2009; Cheng et al. 2014).

$T_m'$  is unique to food and is closely related to the molecular weight of the total solids present in the foods. In Table 4, the  $T_m'$  of both the SD and FD egg white decreased with increasing solids content. The decreasing trend of  $T_m'$  was similar to that of  $T_F$  for the egg white. Figure 8 presents the freezing curve, which was predicted by fitting Eq. (4). The model parameter  $E$  was calculated using a non-linear fitting method and determined to be 0.045 and 0.056 for the SD and FD egg whites, respectively. Based on the value of  $E$ , the effective molecular weight of the solids was 400.0 and 321.4 for the SD and FD egg whites, respectively. The effective molecular weight of the solids calculated for the SD egg white was similar to the FD egg white. In Fig. 8, the  $(T_m')_u$  at the unfreezable water content ( $X_w'$ ) was calculated as  $-11.3$  °C and  $-17.9$  °C by extrapolating the freezing curve up to  $X_s'$  (i.e., maximally freeze-concentrated solutes,  $X_s' = 1 - X_w'$ ) of 0.717 and 0.772 g solids/g sample (w.b.) for the SD and FD egg whites, respectively. The  $(T_m')_u$  values obtained for the egg white samples were similar to other protein foods, including  $-17.4$  °C at 0.688 g solids/g sample (w.b.) for king fish (Sablani et al. 2007),  $-18.1$  °C at 0.680 g solids/g sample (w.b.) for abalone (Sablani et al. 2004), and  $-13.3$  °C at 0.610 g solids/g sample (w.b.) for tuna (Rahman et al. 2003). The  $(T_m')_u$  of FD egg white was less than that of the SD egg white because the  $T_F$  of the samples decreased with increasing soluble solids content, and thus, a higher  $X_s'$  value of the FD egg white led to a lower  $(T_m')_u$  of the FD samples. This result was consistent with the significantly lower values of  $T_F$  in the FD egg white at  $X_s$  above 0.68 g solids/g sample (w.b.) (close to  $X_s'$  value) in Fig. 8 and Table 4.

**Table 4** Thermal transitions and maximal-freeze-concentration conditions of egg white containing freezable water

| Samples | $X_s$ (g/g (w.b.)) | $T_m'$ (°C)       | $T_{gi}$ (°C) | $T_{gm}$ (°C) | $T_{ge}$ (°C) | $T_F$ (°C)        | $\Delta H_m$ (J/g (w.b.)) |
|---------|--------------------|-------------------|---------------|---------------|---------------|-------------------|---------------------------|
| SD      | 0.68               | $-22.7 \pm 1.5e$  | —             | —             | —             | $-11.2 \pm 0.81e$ | $16.4 \pm 1.2e$           |
|         | 0.56               | $-16.0 \pm 1.3d$  | —             | —             | —             | $-4.72 \pm 0.30d$ | $64.1 \pm 1.7d$           |
|         | 0.46               | $-14.4 \pm 0.8c$  | —             | —             | —             | $-2.64 \pm 0.21c$ | $106.1 \pm 3.3c$          |
|         | 0.36               | $-12.7 \pm 0.9b$  | —             | —             | —             | $-1.30 \pm 0.07b$ | $145.1 \pm 0.1b$          |
|         | 0.28               | $-10.5 \pm 0.6a$  | —             | —             | —             | $-0.75 \pm 0.06a$ | $182.6 \pm 1.1a$          |
| FD      | 0.69               | $-26.9 \pm 3.2d$  | —             | —             | —             | $-15.5 \pm 1.3d$  | $18.7 \pm 1.2d$           |
|         | 0.55               | $-16.8 \pm 3.7c$  | —             | —             | —             | $-3.86 \pm 0.33c$ | $69.6 \pm 4.2c$           |
|         | 0.46               | $-15.0 \pm 0.6bc$ | —             | —             | —             | $-2.53 \pm 0.10b$ | $97.9 \pm 3.9b$           |
|         | 0.37               | $-13.4 \pm 1.1ab$ | —             | —             | —             | $-1.41 \pm 0.13a$ | $134.5 \pm 5.6a$          |
|         | 0.27               | $-11.6 \pm 0.7a$  | —             | —             | —             | $-0.99 \pm 0.04a$ | $139.4 \pm 6.4a$          |

Each value is written as mean  $\pm$  SD ( $n = 3$ )

—: Not detectable

Different small letters (a–e) within the same column represent significant difference ( $P < 0.05$ )

### Conclusions

The thermal transition temperatures of spray-dried (SD) and freeze-dried (FD) egg whites were investigated by DSC. For egg white samples containing unfreezable water (lower water contents), the glass transition temperatures ( $T_g$ ) ranging from 112.0 to 85.3 °C of the SD egg whites were detected at water contents ( $X_w$ ) ranging from 0.039 to 0.093 g water/g sample (w.b.). This result showed that the quality stability of egg white can be maintained if it was dried at a temperature lower than its  $T_g$  at the corresponding  $X_w$ . The denaturation temperatures ( $T_d$ ) of ovotransferrin and ovalbumin in the SD samples were obtained when  $X_w$  ranged from 0.082 to 0.143 g water/g sample (w.b.) and 0.039 to 0.282 g water/g sample (w.b.), respectively. However, only the  $T_d$  of ovotransferrin and ovalbumin were observed, and no  $T_g$  was traced in the FD

samples containing unfreezable water content (0.043–0.206 g water/g sample (w.b.)).

For the SD and FD egg white samples containing freezable water (0.32–0.72 and 0.31–0.73 g water/g sample (w.b.) in SD and FD samples), the glass transitions were not detected, and only the freezing points ( $T_F$ ) and end point of freezing ( $T_m'$ ) were observed. The unfreezable water content ( $X_w'$ ) of the SD egg white samples (0.283 g/g (w.b.)) was greater than that of the FD samples (0.228 g/g (w.b.)), as calculated by the enthalpy of ice melting. The characteristic end point of freezing ( $T_m')_u$  of the SD egg white ( $-11.3$  °C) was greater than that of the FD egg white ( $-17.9$  °C) obtained at corresponding unfreezable water contents. When the storage temperatures are above ( $T_m')_u$ , the food matrices become lower viscosity and higher molecular mobility because the frozen matrices are plasticized by melting of ice. Therefore, in order to reduce the rates of quality degradation during frozen storage, the temperature should be below the ( $T_m')_u$  of egg whites.

The heat denaturation of proteins may affect the detection of the glass transition in the DSC curve for egg whites, which caused the different thermal transitions of the SD and FD samples. In addition, the different solubility between SD and FD egg whites was related to the different water-binding capacity of proteins. The different water-binding capacity may cause the different glass-forming systems, and thus leading to the different thermal transitions.

The GAB monolayer water contents for the SD and FD egg whites were similar and obtained to be 0.053 and 0.054 g water/g sample (d.b.), respectively, as the stability criteria based on the water activity concept. The results of thermal transitions and water sorption can be used to design the optimum freezing and drying processes and to predict the stability of egg white in the food industry.

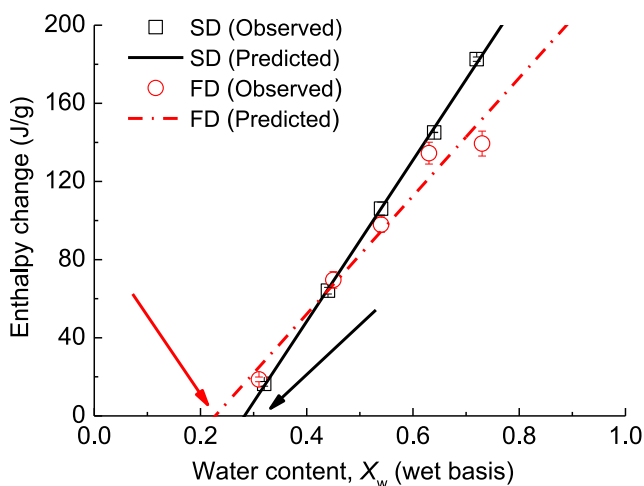


**Fig. 9** Plot of the enthalpy of ice melting as a function of water content in spray-dried and freeze-dried egg white

**Acknowledgments** This work was supported by the National Key Research and Development Program of China (No. 2018YFD0400305). Dr. J. H. Zhao thanks Dr. B. Bhandari and Dr. F. H. Fan for their help in identifying the glass transition. We also would like to thank Dr. Paul McNulty and the reviewers for their constructive comments to improve the manuscript.

## References

- Acevedo, N., Schebor, C., & Buera, M. P. (2006). Water-solids interactions, matrix structural properties and the rate of non-enzymatic browning. *Journal of Food Engineering*, 77(4), 1108–1115.
- AOAC. (2000). *Official methods of analysis* (17th ed.). Gaithersburg: Association of Official Analytical Chemists.
- Ayadi, M. A., Khemakhem, M., Belgith, H., & Attia, H. (2008). Effect of moderate spray drying conditions on functionality of dried egg white and whole egg. *Journal of Food Science*, 73(6), E281–E287.
- Chen, C., Chi, Y. J., & Xu, W. (2012). Comparisons on the functional properties and antioxidant activity of spray-dried and freeze-dried egg white protein hydrolysate. *Food and Bioprocess Technology*, 5(6), 2342–2352.
- Cheng, X. F., Zhang, M., Adhikari, B., & Islam, M. N. (2014). Effect of power ultrasound and pulsed vacuum treatments on the dehydration kinetics, distribution, and status of water in osmotically dehydrated strawberry: a combined NMR and DSC study. *Food and Bioprocess Technology*, 7(10), 1–11.
- Djendoubi Mrad, N., Bonazzi, C., Boudhrioua, N., Kechaou, N., & Courtois, F. (2012). Influence of sugar composition on water sorption isotherms and on glass transition in apricots. *Journal of Food Engineering*, 111(2), 403–411.
- Donovan, J. W., Mapes, C. J., Davis, J. G., & Garibaldi, J. A. (1975). A differential scanning calorimetric study of the stability of egg white to heat denaturation. *Journal of the Science of Food and Agriculture*, 26(1), 73–83.
- Fabra, M. J., Talens, P., Moraga, G., & Martínez-Navarrete, N. (2009). Sorption isotherm and state diagram of grapefruit as a tool to improve product processing and stability. *Journal of Food Engineering*, 93(1), 52–58.
- Ferreira Machado, F., Coimbra, J. S. R., Garcia Rojas, E. E., Minim, L. A., Oliveira, F. C., & Sousa, R. C. S. (2007). Solubility and density of egg white proteins: Effect of pH and saline concentration. *LWT - Food Science and Technology*, 40(7), 1304–1307.
- Gordon, M., & Taylor, J. S. (1952). Ideal copolymers and the second order transitions of synthetic rubbers. I. Non-crystalline copolymers. *Journal of Applied Chemistry*, 2, 493–500.
- Guizani, N., Al-Saidi, G. S., Rahman, M. S., Bornaz, S., & Al-Alawi, A. A. (2010). State diagram of dates: glass transition, freezing curve and maximal-freeze-concentration condition. *Journal of Food Engineering*, 99(1), 92–97.
- Handa, A., Hayashi, K., Shidara, H., & Kuroda, N. (2001). Correlation of the protein structure and gelling properties in dried egg white products. *Journal of Agricultural and Food Chemistry*, 49(8), 3957–3964.
- Haque, M. K., & Roos, Y. H. (2006). Differences in the physical state and thermal behavior of spray-dried and freeze-dried lactose and lactose/protein mixtures. *Innovative Food Science and Emerging Technologies*, 7(1–2), 62–73.
- Harnkarnsujarit, N., Kawai, K., & Suzuki, T. (2015). Effects of freezing temperature and water activity on microstructure, color, and protein conformation of freeze-dried bluefin tuna (*Thunnus orientalis*). *Food and Bioprocess Technology*, 8(4), 916–925.
- Hashimoto, T., Suzuki, T., Hagiwara, T., & Takai, R. (2004). Study on the glass transition for several processed fish muscles and its protein fractions using differential scanning calorimetry. *Fisheries Science*, 70(6), 1144–1152.
- Katekhong, W., & Charoenrein, S. (2017). Color and gelling properties of dried egg white: effect of drying methods and storage conditions. *International Journal of Food Properties*, 20(9), 2157–2168.
- Koç, M., Koç, B., Güngör, Ö., & Ertekin, F. K. (2012). The effect of moisture on physical properties of spray-dried egg powder. *Drying Technology*, 30(6), 567–573.
- Morr, C. V., German, B., Kinsella, J. E., Regenstein, J. M., Van Buren, J. P., Kilara, A., Lewis, B. A., & Mangino, M. E. (1985). A collaborative study to develop a standardized food protein solubility procedure. *Journal of Food Science*, 50(6), 1715–1718.
- Ogolla, J. A., Kulig, B., Bădulescu, L., Okoth, M. W., Esper, G., Breitenbach, J., Hensel, O., & Sturm, B. (2019). Influence of inlet drying air temperature and milk flow rate on the physical, optical and thermal properties of spray-dried camel milk powders. *Food and Bioprocess Technology*, 12(5), 751–768.
- Ohkuma, C., Kawai, K., Viriyarattanasak, C., Mahawanich, T., Tantratian, S., Takai, R., & Suzuki, T. (2008). Glass transition properties of frozen and freeze-dried surimi products: effects of sugar and moisture on the glass transition temperature. *Food Hydrocolloids*, 22(2), 255–262.
- Pelgrom, P. J. M., Schutyser, M. A. I., & Boom, R. M. (2013). Thermomechanical morphology of peas and its relation to fracture behaviour. *Food and Bioprocess Technology*, 6(12), 3317–3325.
- Rahman, M. S. (1995). *Food Properties Handbook* (1st ed.). Boca Raton: CRC Press.
- Rahman, M. S. (2004). State diagram of date flesh using differential scanning calorimetry (DSC). *International Journal of Food Properties*, 7(3), 407–428.
- Rahman, M. S. (2009). Food stability beyond water activity and glass transition: macro-micro region concept in the state diagram. *International Journal of Food Properties*, 12(4), 726–740.
- Rahman, M. S. (2010). Food stability determination by macro-micro region concept in the state diagram and by defining a critical temperature. *Journal of Food Engineering*, 99(4), 402–416.
- Rahman, M. S., Kasapis, S., Guizani, N., & Al-Amri, O. (2003). State diagram of tuna meat: freezing curve and glass transition. *Journal of Food Engineering*, 57(4), 321–326.
- Rahman, M. S., Sablani, S. S., Al-Habsi, N., Al-Maskri, S., & Al-Belushi, R. (2005). State diagram of freeze-dried garlic powder by differential scanning calorimetry and cooling curve methods. *Journal of Food Science*, 70(2), E135–E141.
- Rahman, M. S., Al-Saidi, G., Guizani, N., & Abdullah, A. (2010). Development of state diagram of bovine gelatin by measuring thermal characteristics using differential scanning calorimetry (DSC) and cooling curve method. *Thermochimica Acta*, 509(1–2), 111–119.
- Rahman, M. S., Senadeera, W., Al-Alawi, A., Truong, T., Bhandari, B., & Al-Saidi, G. (2011). Thermal transition properties of spaghetti measured by differential scanning calorimetry (DSC) and thermal mechanical compression test (TMCT). *Food and Bioprocess Technology*, 4(8), 1422–1431.
- Rao, Q. C., & Labuza, T. P. (2012). Effect of moisture content on selected physicochemical properties of two commercial hen egg white powders. *Food Chemistry*, 132(1), 373–384.
- Rao, Q. C., Rocca-Smith, J. R., & Labuza, T. P. (2013a). Storage stability of hen egg white powders in three protein/water dough model systems. *Food Chemistry*, 138(2–3), 1087–1094.
- Rao, Q. C., Fisher, M. C., Guo, M. F., & Labuza, T. P. (2013b). Storage stability of a commercial hen egg yolk powder in dry and intermediate-moisture food matrices. *Journal of Agricultural and Food Chemistry*, 61(36), 8676–8686.
- Roos, Y. H., & Karel, M. (1991). Applying state diagrams to food processing and development. *Food Technology*, 45(12), 66–71.

- Sá, M. M., Figueiredo, A. M., & Sereno, A. M. (1999). Glass transitions and state diagrams for fresh and processed apple. *Thermochimica Acta*, 329(1), 31–38.
- Sablani, S. S., Kasapis, S., Rahman, M. S., Al-Jabri, A., & Al-Habsi, N. (2004). Sorption isotherms and the state diagram for evaluating stability criteria of abalone. *Food Research International*, 37(10), 915–924.
- Sablani, S. S., Rahman, M. S., Al-Busaidi, S., Guizani, N., Al-Habsi, N., Al-Belushi, R., & Soussi, B. (2007). Thermal transitions of king fish whole muscle, fat and fat-free muscle by differential scanning calorimetry. *Thermochimica Acta*, 462(1-2), 56–63.
- Sablani, S. S., Syamaladevi, R. M., & Swanson, B. G. (2010). A review of methods, data and applications of state diagrams of food systems. *Food Engineering Reviews*, 2(3), 168–203.
- Sharma, H. K., Singh, J., Sarkar, B. C., Singh, B., & Premi, M. (2012). Statistical optimization of desugarization process parameters of liquid whole egg using response surface methodology. *LWT - Food Science and Technology*, 47(1), 208–212.
- Shi, Q. L., Zhao, Y., Chen, H. H., Li, Z. J., & Xue, C. H. (2009). Glass transition and state diagram for freeze-dried horse mackerel muscle. *Thermochimica Acta*, 493(1-2), 55–60.
- Shi, Q. L., Wang, X. H., Zhao, Y., & Fang, Z. X. (2012). Glass transition and state diagram for freeze-dried *Agaricus bisporus*. *Journal of Food Engineering*, 111(4), 667–674.
- Shi, Q. L., Lin, W. W., Zhao, Y., & Zhang, P. P. (2015). Thermal characteristics and state diagram of *Penaeus vannamei* meat with and without maltodextrin addition. *Thermochimica Acta*, 616, 92–99.
- Singh, B., & Mehta, S. (2008). Effect of osmotic pretreatment on equilibrium moisture content of dehydrated carrot cubes. *International Journal of Food Science & Technology*, 43(3), 532–537.
- Slade, L., Levine, H., & Reid, D. S. (1991). Beyond water activity: Recent advances based on an alternative approach to the assessment of food quality and safety. *Critical Reviews in Food Science and Nutrition*, 30(2–3), 115–360.
- Sochava, I. V., & Smimova, O. I. (1993). Heat capacity of hydrated and dehydrated globular proteins. Denaturation increment of heat capacity. *Food Hydrocolloids*, 6(6), 513–524.
- Syamaladevi, R. M., Sablani, S. S., Tang, J., Powers, J., & Swanson, B. G. (2009). State diagram and water adsorption isotherm of raspberry (*Rubus idaeus*). *Journal of Food Engineering*, 91(3), 460–467.
- Tironi, V., LeBail, A., & Lamballerie, M. d. (2007). Effects of pressure-shift freezing and pressure-assisted thawing on sea bass (*Dicentrarchus labrax*) quality. *Journal of Food Science*, 72(7), C381–C387.
- Tironi, V., Lamballerie-Anton, M. d., & Le-Bail, A. (2009). DSC determination of glass transition temperature on sea bass (*Dicentrarchus labrax*) muscle: effect of high-pressure processing. *Food and Bioprocess Technology*, 2(4), 374–382.
- Tolstorebrov, I., Eikevik, T. M., & Bantle, M. (2014). Thermal phase transitions and mechanical characterization of Atlantic cod muscles at low and ultra-low temperatures. *Journal of Food Engineering*, 128, 111–118.
- Wang, W., & Zhou, W. B. (2013). Water adsorption and glass transition of spray-dried soy sauce powders using maltodextrins as carrier. *Food and Bioprocess Technology*, 6(10), 2791–2799.
- Zhang, Y., Zhao, J. H., Ding, Y., Xiao, H. W., Sablani, S. S., Nie, Y., Wu, S. J., & Tang, X. M. (2018). Changes in the vitamin C content of mango with water state and ice crystals under state/phase transitions during frozen storage. *Journal of Food Engineering*, 222, 49–53.
- Zhao, J. H., Liu, F., Wen, X., Xiao, H. W., & Ni, Y. Y. (2015). State diagram for freeze-dried mango: freezing curve, glass transition line and maximal-freeze-concentration condition. *Journal of Food Engineering*, 157, 49–56.
- Zhao, J. H., Ding, Y., Nie, Y., Xiao, H. W., Zhang, Y., Zhu, Z., & Tang, X. M. (2016). Glass transition and state diagram for freeze-dried *Lentinus edodes* mushroom. *Thermochimica Acta*, 637, 82–89.
- Zhao, J. H., Ding, Y., Yuan, Y. J., Xiao, H. W., Zhou, C. L., Tan, M. L., & Tang, X. M. (2018). Effect of osmotic dehydration on desorption isotherms and glass transition temperatures of mango. *International Journal of Food Science & Technology*, 53(11), 2602–2609.
- Zhou, B., Zhang, M., Fang, Z. X., & Liu, Y. P. (2014). A combination of freeze drying and microwave vacuum drying of duck egg white protein powders. *Drying Technology*, 32(15), 1840–1847.

**Publisher's Note** Springer Nature remains neutral with regard to jurisdictional claims in published maps and institutional affiliations.